Published in final edited form as:
Science. 2012 October 5; 338(6103): 108–113. doi:10.1126/science.1223821.

Wnt5a Potentiates TGF-β Signaling to Promote Colonic Crypt Regeneration after Tissue Injury

Hiroyuki Miyoshi[1], **Rieko Ajima**[2,§], **Christine Tzy-Yuh Luo**[1], **Terry P. Yamaguchi**[2,*], and **Thaddeus S. Stappenbeck**[1,*]

[1]Department of Pathology and Immunology, Washington University School of Medicine, St. Louis, MO 63110, USA

[2]Cancer and Developmental Biology Laboratory, Center for Cancer Research, National Cancer Institute-Frederick, NIH, Frederick, MD 21702, USA

Re-establishing homeostasis after tissue damage depends on the proper organization of stem cells and their progeny, though the repair mechanisms are unclear. The mammalian intestinal epithelium is well-suited to approach this problem as it is composed of well-delineated units called crypts of Lieberkühn. We found that Wnt5a, a non-canonical Wnt ligand, was required for crypt regeneration after injury in mice. Unlike controls, Wnt5a-deficient mice maintained an expanded population of proliferative epithelial cells in the wound. We found that Wnt5a inhibited proliferation of intestinal epithelial stem cells using an *in vitro* system to enrich for these cells. Surprisingly, the effects of Wnt5a were mediated by activation of transforming growth factor (TGF)-β signaling. These findings suggest a Wnt5a-dependent mechanism for forming new crypt units to re-establish homeostasis.

Tissue regeneration requires proper spatial allocation and organization of new stem cells for efficient return to homeostasis (1, 2). Crypts of Lieberkühn are subunits that house intestinal stem cells and are lost in response to a variety of insults including ischemia, infection, irradiation and inflammatory bowel disease (3). Although individual crypts undergo fission to replicate during homeostasis (fig. S1A) (4, 5), the mechanism of their regeneration is unknown. Thus, crypt regeneration is a proxy for proper stem cell organization and provides an excellent system to uncover new principles underlying stem cell replacement/organization *in vivo*.

To model crypt/epithelial stem cell loss, we previously developed an injury system to focally excise crypts from the absorptive inner lining of the mouse colon (6). In response to the excision of ~1 mm^2 areas from the inner lining of mouse colons (~250-300 crypts), a reproducible program of epithelial alteration occurred. During the first phase (0-4 days post-injury), a flattened layer of non-proliferative epithelial cells (wound-associated epithelial cells; WAE) emanated from crypts adjacent to the wound and migrated over the wound bed surface. During the second phase (4-8 days post-injury), crypts adjacent to the wound formed lateral, open extensions towards the center of the wound bed, forming an array of channel-like structures (fig. S1, B and C). Histologic cross-sections of wound channels at day 6 post-injury showed that they resembled crypts (Fig. 1A) but were distinguished by a predominately proliferative, undifferentiated cell population (Fig. 1B and fig. S1, D and E) (7).

*To whom correspondence should be addressed: Thaddeus S. Stappenbeck, M.D., Ph.D., Department of Pathology and Immunology, Washington University School of Medicine, Box 8118, 660 S. Euclid Avenue, St. Louis, MO 63110, stappenb@pathology.wust.edu; Terry P. Yamaguchi, Ph.D., Cancer and Developmental Biology Laboratory, Center for Cancer Research, National Cancer Institute-Frederick, NIH, Frederick, MD 21702, yamagute@mail.nih.gov.
§Current address: Developmental Genetics Group, Graduate School of Frontier Biosciences, Osaka University, Osaka 565-0871 Japan

We hypothesized that new crypts within wounds arose from existing crypts adjacent to the wound bed (6). We therefore performed lineage tracing experiments using *Vil*-CreERT: *Gtrosa26*^{tm1Sor} (*Rosa26R*) mice (8, 9). To mark a subset of crypts prior to injury, we activated Cre recombinase in the intestinal epithelium with a single tamoxifen injection followed by a one week delay. Four days post-injury in these mice, coherent columns of LacZ-positive WAE cells emanated from adjacent crypts towards the wound center (Fig. 1C and fig. S2A) (6). At day 8 post-injury, distinctive LacZ-positive epithelial channels emanated from adjacent crypts towards the center of the wound (Fig. 1, C and D and fig. S2A). At later time points (14 and 28 days post-injury), clusters of LacZ-positive crypts were located within the original wound bed site (Fig. 1, C and E). Sections of these LacZ-positive crypts showed a return to homeostasis; differentiated epithelial cells (i.e. goblet cells) were present in the upper crypt similar to crypts in non-wounded areas (fig. S2B). These experiments showed that new colonic crypts can originate from crypts adjacent to the wound site and suggest that epithelial stem cells migrated through distinctive channels to enter the wound bed (fig. S2C).

At day 6 post-injury, we readily observed multiple invaginations of wound channels suggesting that multiple fission events occurred to produce new crypts (Fig. 1A). Comparison of transcript abundance (10) of budding wound channels (day 6 post-injury) to crypts in uninjured areas showed that the wound channel epithelium contained highly proliferative cells (fig. S3A) enriched in Wnt signaling transcripts (canonical and non-canonical combined) (fig. S3, A and B). As canonical Wnt signaling is critical for intestinal stem cell homeostasis (11-14) and non-canonical Wnt signaling plays a role in intestinal development (15), we screened expression of 19 Wnt ligands and 4 R-spondin co-activators by RT-PCR (fig. S3C). Interestingly, mRNAs encoding the non-canonical Wnt ligand Wnt5a were significantly enriched in the wound bed compared to the adjacent uninjured mucosa (Fig. 2, A and B; fig. S3, D and E).

Non-canonical Wnts expressed in undifferentiated mesenchymal cells affect tissue regeneration in hydra and zebrafish (16, 17). Similarly, *in situ* hybridization showed an expanded population of Wnt5a-positive stromal cells in the colonic wound bed (Fig. 2C and fig. S4) compared to uninjured mucosa (Fig. 2C) (18). Importantly, a sub-population of Wnt5a-positive cells localized near wound channels. Similar to other injury models, the Wnt5a-positive stromal cells in the colonic wound bed did not express markers of differentiation including α-smooth muscle actin, (myofibroblasts) or β-catenin (endothelial cells) (fig. S5, A and B). Interestingly, we noted an additional subpopulation of Wnt5a-positive cells beneath the mucosal wound bed in the serosal area (fig. S6A). During development, one potential source of undifferentiated stromal progenitor cells in the mouse intestine is mesothelial cells that form the serosa (the outer surface of the intestinal tube) (19). We performed a genetic lineage tracing experiment for mesothelial cells using WT1^{CreERT2}: *Rosa26R* mice (20). Tamoxifen injection activates Cre recombinase in mesothelial cells that in turn marks these cells by LacZ. A population of Wnt5a-positive cells was derived from these WT1-marked cells at day 6 post-injury (fig. S6, B to E) suggesting Wnt5a-positive cells are in part derived from mesothelial cells.

We next examined the association of Wnt5a-positive cells with wound channel epithelial cells. During injury repair, wound channels were comprised of an expanded population of proliferative (Ki-67-positive), canonical Wnt-active (Axin2-positive; 21) epithelial cells. Strikingly, Wnt5a-positive cells localized to clefts at the base of wound channels, suggesting areas of nascent crypt formation (Fig. 2D). In addition, Wnt5a-positive cells also were located adjacent to non-proliferative wound channel epithelial cells (Fig. 2E). This was specific for wound channels, as in uninjured areas, Wnt5a-positive mesenchymal cells were not associated with crypt bases that contain canonical Wnt-active epithelial cells (Fig. 2D).

These results suggested that Wnt5a-positive mesenchymal cells may induce new crypt formation by locally inhibiting proliferation of the stem/progenitor cell population within the wound channel.

To test this hypothesis *in vivo*, we generated a *Wnt5a* conditional knockout allele (fig. S7, A-D). We crossed $Wnt5a^{flox}$ mice with CAGGCreER™ (22) or Ubc-Cre-ER^{T2} (23) transgenic mice for global cellular targeting and generated CreERT-expressing $Wnt5a^{flox/flox}$ mice ($Wnt5a^{ko/ko}$) as well as CreERT-expressing $Wnt5a^{flox/+}$ and $Wnt5a^{+/+}$ mice (controls). After serial tamoxifen injections to activate Cre recombinase, we created colonic mucosal injuries and analyzed repair. $Wnt5a^{ko/ko}$mice generated by both methods contained normal appearing WAE cells (fig. S7E), but contained abnormal wound channels at day 6 and 8 post-injury. As compared to uninjured controls, at day 6 post-injury, $Wnt5a^{ko/ko}$ wound channels contained significantly fewer invaginations (Fig. 2, F and G) and at day 8 post-injury, they did not develop into new crypt-like structures (Fig. 2H). These results showed that Wnt5a has a crucial role in the proper formation and eventual subdivision of wound channels into crypts (Fig. 2I).

To test the direct effects of Wnt5a on wound channel epithelium, we established an *in vitro* culture system that mimicked wound channels. Conditioned media from an L cell line expressing Wnt3a, R-spondin3 and noggin (L-WRN) (11, 13, 14) maintained highly proliferative, epithelial colonic stem/progenitor cells (Lgr5-positive; 24) as organoid spheres in culture (fig. S8, tables S2 and S3); these properties were similar to *in vivo* wound channel epithelial cells. Interestingly, Wnt5a-soaked beads (fig. S9) induced clefts within colonic organoids more frequently than control beads (Fig. 3, A and B). Epithelial proliferation in areas of contact with Wnt5a-soaked beads was suppressed compared to control beads (Fig. 3C). Furthermore, addition of Wnt5a to the organoid culture medium suppressed colonic sphere formation stimulated by Wnt3a and R-spondin1 (Fig. 3D). Wnt5a decreased Ki-67 and Lgr5 expression in a dose-dependent manner (fig. S10A). However, Axin2 expression was not suppressed by Wnt5a (fig. S10A), in contrast to previous findings that suggest Wnt5a antagonizes canonical Wnt signaling (25-28). The connection between non-canonical Wnt signaling and the cell cycle is unclear. Increased expression of cyclin-dependent kinase (Cdk) inhibitors can inhibit epithelial proliferation. We found that Wnt5a increased expression of multiple Cdk inhibitors, most notably $p15^{INK4B}$ (Cdkn2b) in treated colonic epithelial organoids (fig. S10B). These results show that a focal source of non-canonical Wnt initiates a critical intermediary step to reestablish homeostasis of the colonic epithelium.

Because $p15^{INK4B}$ expression can be induced by TGF-β (29), a classical inhibitor of epithelial proliferation (30), we tested if Wnt5a activated the TGF-β signaling pathway. In colonic organoids, recombinant TGF-β1 suppressed proliferation and induced Serpine1 (PAI-1) expression indicating Smad transactivation (31) downstream of the TGF-β type 1 receptor (fig. S11, A and B). Surprisingly, Wnt5a also stimulated Serpine1expression in a dose dependent manner (Fig. 4A) and enhanced Smad3 phosphorylation/nuclear localization (Fig. 4B). In injured $Wnt5a^{ko/ko}$ as compared to control mice, the loss of Wnt5a expression was associated with diminished phosphorylation of Smad3 in the stem/progenitor population at the base of wound channels (Fig. 4, C and D and fig. S11, C and D). The action of Wnt5a required kinase activity of the TGF-β receptor as SB431542, a kinase inhibitor for TGF-β type 1 receptor, suppressed all Wnt5a effects on cell growth as well as Ki-67 and Serpine1 expression (Fig. 4E and fig S11E). Thus, Wnt5a expression is required to potentiate TGF-β signaling at the base of wound channels and mimicked the effects of Wnt5a *in vitro*.

Despite sharing several similar components, the canonical and non-canonical Wnt signaling pathways utilize distinct co-receptors, LRP5/6 and ROR1/2, respectively, (32). Intestinal

organoids exclusively expressed Ror2 (fig. S12) and *Ror2*$^{-/-}$and *Wnt5a*$^{-/-}$ mice similarly display defective gut elongation (15, 33). Using colonic organoids with shRNA knockdown of Ror2 (fig. S13, A-C), we found that Wnt5a and TGF-β1showed diminished Serpine1induction (Fig. 4F) indicating that the activation of the TGF-β signaling pathway by Wnt5a was mediated through Ror2. Interestingly, Ror2 knockdown did not affect growth inhibition of Wnt5a and TGF-β1 (fig. S14), suggesting that TGF-β inhibited the cell cycle in a transcription-independent manner as previously described (34) and that the signaling through Ror1/2 enhanced transcriptional activity of the Smad protein complex. Although the core components of the TGF-β signaling pathway consisting of type I and II receptors and Smad proteins are relatively simple, regulatory mechanisms, including protein modification and translocation, are highly complex (35). This experimental system will help identify more precise molecular mechanisms of cell cycle inhibition by non-canonical Wnt and TGF-β.

Here we show that wound channels are a critical intermediate structure during colonic epithelial wound repair. These channels undergo Wnt5a-mediated subdivision that utilizes a novel mechanism to potentiate TGF-β signaling. The effects of Wnt5a are primarily mediated by focal inhibition of proliferation, though we cannot rule out effects on cell polarity/asymmetric cell division. The process of crypt regeneration appears to re-utilize elements of a fetal developmental program (15, 36). Even though a colonic mesenchymal niche is not yet defined, our findings suggest that Wnt5a-positive cells are a critical part of this niche during injury repair as they affect the organization of the regenerating epithelium. We propose that such epithelial-mesenchymal interactions during repair will occur in other tissues and organisms (1) such as hair follicles that elevate specific Wnt family members during regeneration (37).

Supplementary Material

Refer to Web version on PubMed Central for supplementary material.

Acknowledgments

We thank R. Kopan for comments on the manuscript. We thank W. Pu for reagents. We thank R. Head and C. Storer for the microarray analysis. This work was funded by the NIH (DK90251), the Pew Scholars Program in the Biomedical Sciences, 5T35DK074375 (Trans-NIDDK Short-Term Training for Medical Students), the Washington University Digestive Disease Research Core (NIH P30-DK52574), and the Intramural Research Program of the NIH, National Cancer Institute, Center for Cancer Research. Microarray data is available on Array Express (accession # E-MTAB-1175). MTAs will be required for the acquisition of the *Wnt5a*$^{f/f}$ mice from the National Cancer Institute and the L-WRN cell line from the Washington University Medical School. The data presented in this manuscript are tabulated in the main paper and the supplementary materials.

References and Notes

1. Stappenbeck TS, Miyoshi H. The role of stromal stem cells in tissue regeneration and wound repair. Science. 2009; 324:1666–1669. [PubMed: 19556498]
2. Lanza, R., editor. Essentials of Stem Cell Biology. 2. Elsevier; San Diego, CA: 2009.
3. Walker MR, Patel KK, Stappenbeck TS. The stem cell niche. J Pathol. 2009; 217:169–180. [PubMed: 19089901]
4. Chang WW, Leblond CP. Renewal of the epithelium in the descending colon of the mouse. II. Renewal of argentaffin cells. Am J Anat. 1971; 131:101–109. [PubMed: 4103770]
5. Park HS, Goodlad RA, Wright NA. Crypt fission in the small intestine and colon. A mechanism for the emergence of G6PD locus-mutated crypts after treatment with mutagens. Am J Pathol. 1995; 147:1416–1427. [PubMed: 7485404]
6. Seno H, et al. Efficient colonic mucosal wound repair requires Trem2 signaling. Proc Natl Acad Sci USA. 2009; 106:256–261. [PubMed: 19109436]

7. Pull SL, Doherty JM, Mills JC, Gordon JI, Stappenbeck TS. Activated macrophages are an adaptive element of the colonic epithelial progenitor niche necessary for regenerative responses to injury. Proc Natl Acad Sci USA. 2005; 102:99–104. [PubMed: 15615857]
8. el Marjou F, et al. Tissue-specific and inducible Cre-mediated recombination in the gut epithelium. Genesis. 2004; 39:186–193. [PubMed: 15282745]
9. Soriano P. Generalized lacZ expression with the ROSA26 Cre reporter strain. Nat Genet. 1999; 21:70–71. [PubMed: 9916792]
10. Cadwell K, et al. Virus-plus-susceptibility gene interaction determines Crohn's disease gene Atg16L1 phenotypes in intestine. Cell. 2010; 141:1135–1145. [PubMed: 20602997]
11. Sato T, et al. Single Lgr5 stem cells build crypt-villus structures in vitro without a mesenchymal niche. Nature. 2009; 459:262–265. [PubMed: 19329995]
12. Ootani A, et al. Sustained *in vitro* intestinal epithelial culture within a Wnt-dependent stem cell niche. Nat Med. 2009; 15:701–706. [PubMed: 19398967]
13. Sato T, et al. Long-term expansion of epithelial organoids from human colon, adenoma, adenocarcinoma, and Barrett's epithelium. Gastroenterology. 2011; 141:1762–1772. [PubMed: 21889923]
14. Jung P, et al. Isolation and in vitro expansion of human colonic stem cells. Nat Med. 2011; 17:1225–1227. [PubMed: 21892181]
15. Cervantes S, Yamaguchi TP, Hebrok M. Wnt5a is essential for intestinal elongation in mice. Dev Biol. 2009; 326:285–294. [PubMed: 19100728]
16. Philipp I, et al. Wnt/β-catenin and noncanonical Wnt signaling interact in tissue evagination in the simple eumetazoan. Hydra Proc Natl Acad Sci USA. 2009; 106:4290–4295.
17. Stoick-Cooper CL, et al. Distinct Wnt signaling pathways have opposing roles in appendage regeneration. Development. 2007; 134:479–489. [PubMed: 17185322]
18. Gregorieff A, et al. Expression pattern of Wnt signaling components in the adult intestine. Gastroenterology. 2005; 129:626–638. [PubMed: 16083717]
19. Wilm B, Ipenberg A, Hastie ND, Burch JBE, Bader DM. The serosal mesothelium is a major source of smooth muscle cells of the gut vasculature. Development. 2005; 132:5317–5328. [PubMed: 16284122]
20. Zhou B, et al. Epicardial progenitors contribute to the cardiomyocyte lineage in the developing heart. Nature. 2008; 454:109–113. [PubMed: 18568026]
21. Lustig B, et al. Negative feedback loop of Wnt signaling through upregulation of conductin/axin2 in colorectal and liver tumors. Mol Cell Biol. 2002; 22:1184–1193. [PubMed: 11809809]
22. Hayashi S, McMahon AP. Efficient recombination in diverse tissues by a tamoxifen-inducible form of Cre: a tool for temporally regulated gene activation/inactivation in the mouse. Dev Biol. 2002; 244:305–318. [PubMed: 11944939]
23. Ruzankina Y, et al. Deletion of the developmentally essential gene ATR in adult mice leads to age-related phenotypes and stem cell loss. Cell Stem Cell. 2007; 1:113–126. [PubMed: 18371340]
24. Barker N, et al. Identification of stem cells in small intestine and colon by marker gene *Lgr5*. Nature. 2007; 449:1003–1007. [PubMed: 17934449]
25. Topol L, et al. Wnt-5a inhibits the canonical Wnt pathway by promoting GSK-3-independent beta-catenin degradation. J Cell Biol. 2003; 162:899–908. [PubMed: 12952940]
26. Mikels AJ, Nusse R. Purified Wnt5a protein activates or inhibits beta-catenin-TCF signaling depending on receptor context. PLoS Biol. 2006; 4:e115. [PubMed: 16602827]
27. Sato A, Yamamoto H, Sakane H, Koyama H, Kikuchi A. Wnt5a regulates distinct signalling pathways by binding to Frizzled2. EMBO J. 2010; 29:41–54. [PubMed: 19910923]
28. Ishitani T, et al. The TAK1-NLK mitogen-activated protein kinase cascade functions in the Wnt-5a/Ca^{2+} pathway to antagonize Wnt/β-catenin signaling. Mol Cell Biol. 2003; 23:131–139. [PubMed: 12482967]
29. Hannon GJ, Beach D. $p15^{INK4B}$ is a potential effector of TGF-β-induced cell cycle arrest. Nature. 1994; 371:257–261. [PubMed: 8078588]
30. Moses HL, Yang EY, Pietenpol JA. TGF-β stimulation and inhibition of cell proliferation: new mechanistic insights. Cell. 1990; 63:245–247. [PubMed: 2208284]

31. Dennler S, et al. Direct binding of Smad3 and Smad4 to critical TGFβ-inducible elements in the promoter of human plasminogen activator inhibitor-type 1 gene. EMBO J. 1998; 17:3091–3100. [PubMed: 9606191]
32. Grumolato L, et al. Canonical and noncanonical Wnts use a common mechanism to activate completely unrelated coreceptors. Genes Dev. 2010; 24:2517–2530. [PubMed: 21078818]
33. Yamada M, et al. Ror2 is required for midgut elongation during mouse development. Dev Dyn. 2010; 239:941–953. [PubMed: 20063415]
34. Iavarone A, Massagué J. Repression of the CDK activator Cdc25A and cell-cycle arrest by cytokine TGF-β in cells lacking the CDK inhibitor p15. Nature. 1997; 387:417–422. [PubMed: 9163429]
35. Gough NR. Focus issue: an expanding world for TGF-β signaling. Sci Signal. 2008; 1:eg8. [PubMed: 19018010]
36. Yamaguchi TP, Bradley A, McMahon AP, Jones S. A Wnt5a pathway underlies outgrowth of multiple structures in the vertebrate embryo. Development. 1999; 126:1211–1223. [PubMed: 10021340]
37. Ito M, et al. Wnt-dependent de novo hair follicle regeneration in adult mouse skin after wounding. Nature. 2007; 447:316–320. [PubMed: 17507982]
38. Liu P, Jenkins NA, Copeland NG. A highly efficient recombineering-based method for generating conditional knockout mutations. Genome Research. 2003; 13:476–484. [PubMed: 12618378]
39. Tessarollo L. Manipulating mouse embryonic stem cells. Methods Mol Biol. 2001; 158:47–63. [PubMed: 11236671]
40. Huh WJ, Mysorekar IU, Mills JC. Inducible activation of Cre recombinase in adult mice causes gastric epithelial atrophy, metaplasia, and regenerative changes in the absence of “floxed” alleles. Am J Physiol Gastrointest Liver Physiol. 2010; 299:G368–380. [PubMed: 20413717]
41. Alien ND, et al. Transgenes as probes for active chromosomal domains in mouse development. Nature. 1988; 333:852–855. [PubMed: 3386733]
42. Wong MH, Hermiston ML, Syder AJ, Gordon JI. Forced expression of the tumor suppressor adenomatosis polyposis coli protein induces disordered cell migration in the intestinal epithelium. Proc Natl Acad Sci USA. 1996; 93:9588–9593. [PubMed: 8790374]
43. Huang DW, Sherman BT, Lempicki RA. Systematic and integrative analysis of large gene lists using DAVID bioinformatics resources. Nature Protoc. 2009; 4:44–57. [PubMed: 19131956]
44. Dennis G, et al. DAVID: Database for Annotation, Visualization, and Integrated Discovery. Genome Biol. 2003; 4:R60.
45. Willert K, et al. Wnt proteins are lipid-modified and can act as stem cell growth factors. Nature. 2003; 423:448–452. [PubMed: 12717451]
46. Watanabe K, et al. A ROCK inhibitor permits survival of dissociated human embryonic stem cells. Nat Biotechnol. 2007; 25:681–686. [PubMed: 17529971]
47. Manieri, NA.; Drylewicz, MR.; Miyoshi, H.; Stappenbeck, TS. Igf2bp1 is required for full induction of *Ptgs2* mRNA in colonic mesenchymal stem cells in mice. Gastroenterology. in press (available at http://dx.doi.org/10.1053/j.gastro.2012.03.037)
48. Lefebvre O, et al. The mouse one P-domain (*pS2*) and two P-domain (*mSP*) genes exhibit distinct patterns of expression. J Cell Biol. 1993; 122:191–198. [PubMed: 8314841]
49. James R, Kazenwadel J. Homeobox gene expression in the intestinal epithelium of adult mice. J Biol Chem. 1991; 266:3246–3251. [PubMed: 1671571]
50. James R, Erler T, Kazenwadel J. Structure of the murine homeobox gene *cdx-2*. Expression in embryonic and adult intestinal epithelium. J Biol Chem. 1994; 269:15229–15237. [PubMed: 7910823]
51. Markowitz AJ, Wu GD, Birkenmeier EH, Traber PG. The human sucrase-isomaltase gene directs complex patterns of gene expression in transgenic mice. Am J Physiol Gastrointest Liver Physiol. 1993; 265:G526–G539.
52. Sowden J, Leigh S, Talbot I, Delhanty J, Edwards Y. Expression from the proximal promoter of the carbonic anhydrase 1 gene as a marker for differentiation in colon epithelia. Differentiation. 1993; 53:67–74. [PubMed: 8359594]

53. Zhou L, Lim L, Costa RH, Whitsett JA. Thyroid transcription factor-1, hepatocyte nuclear factor-3β, surfactant protein B, C, and Clara cell secretory protein in developing mouse lung. J Histochem Cytochem. 1996; 44:1183–1193. [PubMed: 8813084]

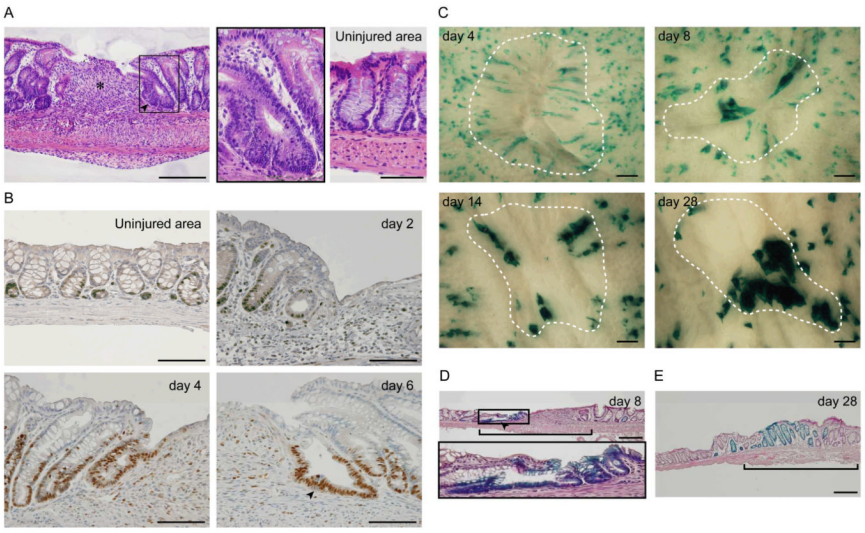

Fig. 1.

Colonic crypts regenerate from existing crypts during injury repair. (**A**) An H&E–stained section of a wound at day 6 post-injury. An asterisk indicates the center of the wound bed. An arrowhead indicates a wound channel that consists of immature epithelial cells (boxed region, see inset). Crypts distant from the wound site are represented in the panel labeled 'Uninjured area'. Bar, 200 μm. (**B**) Sections stained for Ki-67 (brown) to label proliferative cells at various time points after biopsy injury. An arrowhead labels the wound channel at day 6 post-injury. Bars, 100 μm. n=3 wounds/time point for (A) and (B). (**C**) Migration of clonal cell populations from labeled crypts after wounding in *Vil*-CreERT: *Rosa26R* mice. Cells expressing LacZ were visualized by the staining with 5bromo-4-chloro-3-indolyl-β-D-galactoside (X-gal). Dotted lines outline original wound area. Bars, 200 μm. (**D**) An H&E–stained section of a wound at day 8 post-injury in a *Vil*-CreERT: *Rosa26R* mouse. LacZ-positive cells (blue) were present in a wound channel (arrowhead; see inset). The wound bed is delineated by a bracket. Bar, 200 μm. (**E**) An H&E–stained section of a wound at day 28 post-injury in a *Vil*-CreERT: *Rosa26R* mouse shows clusters of LacZ-positive crypts in the wound bed (defined by bracket). Bar, 200 μm. n=6 wounds/time point for (C), (D) and (E).

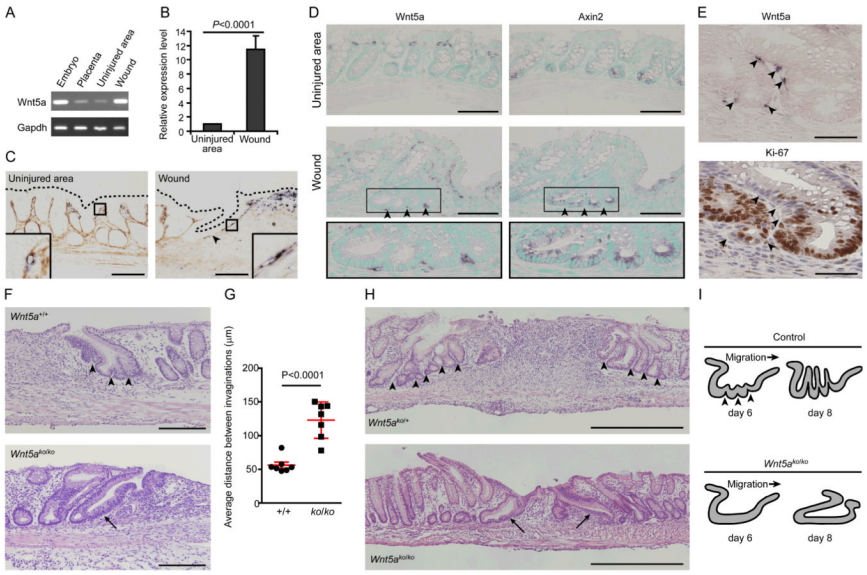

Fig. 2.

Wnt5a-positive mesenchymal cells stimulate crypt regeneration after injury. (**A**) RT-PCR analysis of Wnt5a from RNAs isolated from an E13.5 embryo and its placenta tissue (controls), the wound bed and adjacent uninjured mucosa. (**B**) Plots of mean (+SD) relative Wnt5a mRNA expression levels as determined by quantitative RT-PCR analysis of wound beds and adjacent uninjured mucosa at day 4 post-injury. Data were analyzed using Student's *t*-test (n=4/group). (**C**) Mouse colon sections at day 6 post-injury (uninjured area and wound) stained by *in situ* hybridization for Wnt5a (purple) and hyaluronic acid (basement membrane, brown). Dotted lines outline the apical epithelial surface. Bars, 100 μm. (**D**) Serial sections of uninjured area and a colonic wound at day 6 post-injury stained for Wnt5a and Axin2 mRNA, respectively. Arrowheads indicate Wnt5a-positive cells associated with wound channel clefts (insets). Methyl green labeled nuclei. Bars, 100 μm. (**E**) Serial sections of a colonic wound channel at day 6 post-injury stained for Wnt5a mRNA (left) and Ki-67 (right). Wnt5a-positive cells were localized near quiescent epithelial cells (arrowheads). Sections were counterstained with nuclear fast red (left) and hematoxylin (right). Bars, 100 μm. n=3 wounds/assay. (**F**) Sections from a *CAGGCreER*^{TM}*:Wnt5a*$^{+/+}$ (*Wnt5a*$^{+/+}$) mouse and a *CAGGCreER*^{TM}*:Wnt5a*$^{flox/flox}$ (*Wnt5a*$^{ko/ko}$) mouse at day 6 post-injury stained by H&E. Arrowheads indicate wound channel invaginations. The arrow indicates an immature wound channel without invaginations. Bars, 200 μm. (**G**) Graph of the average distance between wound channel invaginations (± SD) (n=7/group). Each dot represents the average distance for an individual wound channel. Data were analyzed using Student's *t*-test. (**H**) H&E-stained sections from an *Ubc-CreERT2:Wnt5a*$^{flox/+}$ (*Wnt5a*$^{ko/+}$) and *Ubc-Cre-ER*^{T2}*:Wnt5a*$^{flox/flox}$ (*Wnt5a*$^{ko/ko}$) mouse at day 8 post-injury (n=3 mice analyzed/group). Arrowheads indicate the space between crypt-like structures that developed from wound channels. Arrows indicate abnormal immature wound channels with no crypt-like structures. Bars, 500 μm. (**I**) Schematic diagrams of defect in crypt regeneration in *Wnt5a*$^{ko/ko}$ mice.

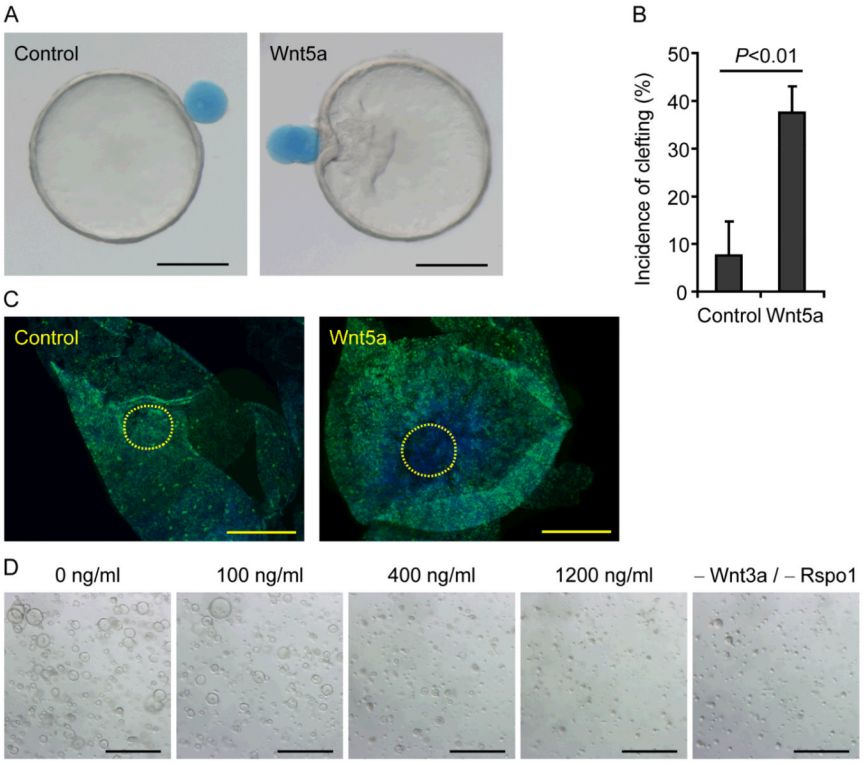

Fig. 3.

Wnt5a inhibits proliferation of colonic epithelial stem cells. (**A**) Focal Wnt5a-induced clefts in colonic epithelial organoids. A control (left panel) or a Wnt5a-soaked bead (right panel) was placed adjacent to different colonic organoids. Bars, 200 μm. (**B**) Plot of the mean cleft incidence of colonic organoids (+ SD) attached to control or Wnt5a-soaked beads (n=3 experiments). A Student's t-test was used to determine significance. (**C**) Colonic organoids attached to either control (left panel) or Wnt5a-soaked beads (right panel) were stained for Ki-67 (green). Yellow dotted lines outline the bead attachment area. Nuclei were counterstained with bis-benzimide (blue). Representative images from 3 samples (per group) were shown. Bars, 200 μm. (**D**) Representative images of colonic epithelial organoids cultured for 48 hours in indicated conditions (n=3 experiments). Bars, 500 μm.

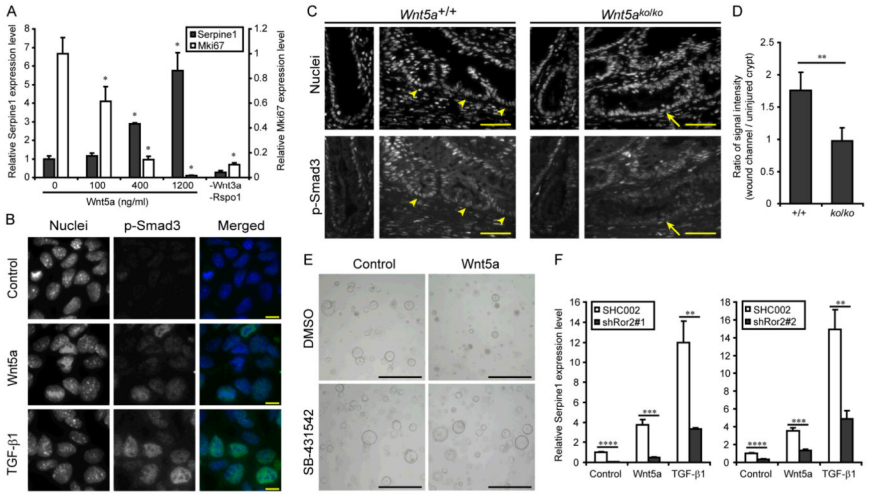

Fig. 4.

Wnt5a activates TGF-β signaling pathway. (**A**) Colonic organoids were cultured for 24 hours with recombinant Wnt5a. Plots of mean (+ SD) relative mRNA expression levels of Serpine1 and Mki67 were determined by quantitative RT-PCR analysis (n=3/group). Data were analyzed using one-way ANOVA followed by Tukey's test (P<0.0001). The asterisk indicates differences compared to the baseline condition (0 ng/ml) that were significant (P<0.05) in the post test. (**B**) Nuclear localization of p-Smad3 protein. Colonic epithelial cells grown on Matrigel coated chambers were incubated without ligands (control) and with either Wnt5a (400 ng/ml) or TGF-β1 (1 ng/ml) for 2 hours and then fixed and stained for p-Smad3 (representative images from three experiments). Bars, 10 μm. (**C**) Distribution of p-Smad3 in the wound channels (right panels) and uninjured crypt units (left panels). Colonic sections from *Ubc-Cre-ER*^{T2}: Wnt5a$^{+/+}$ (Wnt5a$^{+/+}$) and *Ubc-Cre-ER*^{T2}: *Wnt5a*$^{flox/flox}$(*Wnt5a*$^{ko/ko}$) wounds at day 6 post-injury were stained for p-Smad3 (bottom panels). Cell nuclei were visualized with bis-benzimide (top panels). Arrowheads and arrows indicated the base of wound channels. Bars, 50 μm. (**D**) Quantification of p-Smad3 in wound channels. Plots of the mean ratio of signal intensity (+ SD) in epithelial cells located in the base of wound channels compared to the base of crypts in unwounded areas (from the same tissue section) were determined as described in Methods (n=4 wounds/group). (**E**) Colonic organoids were cultured for 24 hours without ligands (control) and with Wnt5a (400 ng/ml), SB-431542 (10 μM) or both together. Representative bright field pictures were shown (n=3 experiments). Bars, 500 μm. (**F**) Colonic organoids were cultured for 24 hours without ligands (control) and with Wnt5a (400 ng/ml) and TGF-β1 (1 ng/ml). Two pairs of populations expressing shRNA for independent target sequences and their controls (SHC002) were examined. Plots of mean (+ SD) relative mRNA expression levels were determined by quantitative RT-PCR analysis (n=3/group). The asterisk in (D) and (F) indicates differences that were significant in the Student's t-test. * *P<0.01, * * *P<0.001, * * * *P<0.0001.